Sulfate Complexation of Trivalent Lanthanides Proben by NanoElectrospray Mass Spectrometry and Time-Resolved Laser-Induced Luminescence

Thomas Vercouter,*[†,‡,§,$] Badia Amekraz,*[†] Christophe Moulin,[†] Eric Giffaut,[§] Pierre Vitorge[†,‡]

[†] CEA-DEN Saclay DPC/SECR/LSRM, 91191 Gif-sur-Yvette Cedex, France, [‡] UMR 8587 (same address), [§] Andra, 1/7 rue Jean Monnet, 92298 Châtenay-Malabry Cedex, France

* Authors to whom correspondence should be addressed. Phone: + 33-1-6908-7751. Fax: + 33-1-6908-5411. E-mail: thomas.vercouter@cea.fr; amekraz@cea.fr.

ABSTRACT

Sulfate complexation of lanthanides is of great interest to predict the speciation of radionuclides in natural environments. The formation of $LaSO_4^+(aq)$ in HNO_3/H_2SO_4 aqueous solutions of low ionic strength (I) was studied by nanoElectrospray Ionization - Mass Spectrometry (nanoESI-MS). Several gaseous species containing $LaSO_4^+$ were detected. The formation constant of $LaSO_4^+(aq)$ was determined and extrapolated to $I = 0$ (log $\beta_1° = 3.5 \pm 0.3$) by using a simple Specific Ion interaction Theory (SIT) formula. This value supports the potential of nanoESI-MS for the study of kinetically labile species. The species $La(SO_4)_2^-$ was also detected. Besides, Time-Resolved Laser-Induced Luminescence (TRLIL) was used to study Eu(III) speciation in the ionic conditions 0.02-0.05 M H^+ ($H_2SO_4/HClO_4$) and 0.4-2.0 M Na^+ ($Na_2SO_4/NaClO_4$). The data were interpreted with the species $EuSO_4^+$ (log $\beta_1° = 3.7_8 \pm 0.1$) and $Eu(SO_4)_2^-$ (log $K_2° = 1.5 \pm 0.2$). For extrapolating to $I = 0$ all the major ions were taken into account through several SIT ion-pair parameters, ε. Most of the ε values were estimated by analogy to known parameters for similar ion-pair interactions using linear correlations, while $\varepsilon_{Eu^{3+},SO_4^{2-}} = 0.8_6 \pm 0.5$ was fitted to experimental data, since, to date, SIT coefficients between multi-charged species are not reported. The formation constants here obtained confirm some of those previously measured for Ln(III) and An(III) by various experimental techniques, and conversely do not give credit that in equilibrium conditions TRLIL and other spectroscopic techniques would provide stability constants of only inner sphere complexes. The fluorescence lifetimes measured for $EuSO_4^+$ and $Eu(SO_4)_2^-$ were consistent with the replacement of one H_2O molecule in the first coordination sphere of Eu^{3+} for each added SO_4^{2-} ligand, suggesting a monodentate SO_4^{2-} coordination.

KEYWORDS : lanthanide, inorganic ligand, sulfate, complexation, electrospray, fluorescence.

1. Introduction

Owing to their extensive distribution in natural environments, and their binding capacity towards metal ions, inorganic ligands play a major role in the environmental transport, fate and bioavailability of heavy metals.[1] This raises concern about the possibility of formation of soluble complexes with inorganics, which could modify the migration of long-lived radionuclides released in natural aquifers.[2] The knowledge of radionuclide transport in the geosphere is a key issue for the safety assessment of possible radioactive waste repositories.[3] There is an interest in the determination of thermodynamic data for their interactions with inorganics in order to properly predict their speciation in natural systems.[4] Several trivalent f-block elements represent a significant part of the long-lived radionuclides, typically the actinides (An) Pu, Am, and Cm, and among the lanthanides (Ln), the ^{151}Sm isotope.[5] Moreover analogies between An^{3+} and Ln^{3+} are sometimes used to implement databases.[6] Inorganic ligands can be roughly divided into two distinct groups based on their reactivity for M^{3+} f-element cations and usual concentrations in groundwaters. The first includes the carbonate and hydroxide anions that often form the major complexes with An^{3+} and Ln^{3+} in deep groundwaters; they have been extensively studied.[7-10] The second includes weaker or less abundant ligands, sulfate, phosphate, silicate, chloride, and fluoride anions.[11] Among these latter ones, the sulfate anions deserve particular interest.[11b] In France, an underground laboratory for radioactive waste disposal studies is currently under construction in a Callovo-Oxfordian clay formation, where a sulfate concentration of 0.031 M has recently been proposed for the interstitial waters of the clayey materials.[12] Thus reliable complexation constants are needed to know whether such a concentration could significantly affect the radionuclides speciation. In spite of many years of research, sulfate complexation of An(III) and Ln(III) is still a matter of debate, and so on its consequence on the mobilities of long-lived radionuclides through natural aquifers remains unclear.

Data for the formation of sulfate complexes of trivalent lanthanides have been obtained applying techniques such as conductimetry, solvent extraction, and UV absorption. Table 1 summarizes the stepwise formation constants ($\log \beta_1$ and $\log K_2$) reported in the literature for lanthanum[13-23] and

europium[13,22-31] trivalent ions. Several measurements in the ionic strength range 0.05-2 M have been reported, while some values have been corrected to zero ionic strength and lie between 3.35 and 3.82 for $\log \beta_1°$, and 1.78 and 1.85 for $\log K_2°$. In the case of An(III) complexes, the formation constants that are usually taken into account are the ones selected by the NEA-TDB critical reviews (Thermochemical Data Base project of the Nuclear Energy Agency OECD):[9,10] $\log \beta_1° = 3.85\pm0.03$ and $\log K_2° = 1.5\pm0.7$ have been selected by Silva *et al.* in 1995 from experimental data determined by using solvent extraction, ion exchange and electromigration techniques;[9] values for Cm(III) have been provided by such techniques as well as by Time-Resolved Laser-Induced Luminescence (TRLIL), and have been discussed in the recent NEA-TDB updated review.[10] TRLIL has already demonstrated its capacity to obtain reliable speciation data.[32] Paviet *et al.* were the first to use TRLIL in an attempt to directly observe the formation of sulfate complexes, and reported formation constants for the complexes $CmSO_4^+$ and $Cm(SO_4)_2^-$ in 3 mol kg^{-1} NaCl/Na$_2$SO$_4$.[33] In another study by Neck *et al.*, sulfate complexation of Cm(III) was investigated as a function of the ionic strength (0-5.8 mol kg^{-1} NaCl/Na$_2$SO$_4$).[34] However, the values derived from the spectroscopic studies on Cm ($\log \beta_1° = 3.30\pm0.15$ and $\log K_2° = 0.40\pm0.15$) have been selected by the authors of the NEA-TDB updated review, and appeared to be significantly lower than those previously selected for Am: 3.30 and 0.40 as compared to 3.85 and 1.5 for $\log \beta_1°$ and $\log K_2°$, respectively.[10] For selecting the new Cm values, it has been argued that ion pairs had been misinterpreted as complexes in the previously reported studies by solution-based methods, leading to incorrect larger formation constants. However, we had already pointed out that spectroscopic techniques provide stability constants that encompass the possible formation of ion pairs,[8] and this will be reported here again; anyhow, in the present study, the data for Eu(III) obtained by a spectroscopic technique (TRLIL) will be compared with results from solution-based methods. The consistency of the analogy between Ln(III) and An(III) in sulfate media will also be checked. It has also been argued in the NEA-TDB updated review that the formation constants reported for Am(III) complexes with inorganics such as carbonate, hydroxide, fluoride, and phosphate are close to, or smaller than those of the corresponding U(VI) complexes.[10,35] Thereby, the selected formation constants for U(VI) sulfate

4

complexes (log $\beta_1° = 3.15\pm0.02$ and log $K_2° = 0.99\pm0.07$) would discredit some values selected for Am(III).[9] However, the proposed correlation does not appear to hold for other ligands such as chloride and nitrate, for which the selected formation constants for U(VI) complexes (log $\beta_1°(UO_2NO_3^+) = 0.30\pm0.15$ and log $\beta_1°(UO_2Cl^+) = 0.17\pm0.02$) are lower than the corresponding Am(III) complexes (log $\beta_1°(AmNO_3^{2+}) = 1.33\pm0.20$ and log $\beta_1°(AmCl^{2+}) = 0.24\pm0.03$).[10,35] These observations likely indicate that making the hypothesis that a common trend for all ions would exist is quite speculative, and therefore it cannot be taken as an indication of the reliability of the spectroscopic data: Such comparisons and analogies are only rough guidelines. The effective charges and ionic radii of Am^{3+} and U in UO_2^{2+} are indeed similar, but the coordination geometries are different since the ligands bound to UO_2^{2+} are located in the plane perpendicular to the linear UO_2-axis.

In this study, thermodynamic methodologies were used together with the advanced spectrometric techniques, TRLIL and nanoElectrospray Ionization - Mass Spectrometry (nanoESI-MS). To date, the coordination chemistry of any lanthanide with sulfate has never been investigated by TRLIL. The combination of spectroscopic information and measurements of species concentrations are much valuable for a speciation purpose. A nanoESI - mass spectrometer was also used to observe the formation of lanthanide sulfate complexes, and determine stability constants. This technique should allow investigations of the aqueous speciation of many elements, providing rapid analyses without constraining sample preparation.

In previous investigations, we have explored ESI-MS potential for metal speciation, and obtained reliable formation constants for Ln(III) complexes with extractant molecules,[36] as well as for thorium hydroxides.[37] However, there are currently two main difficulties encountered in the use of ESI-MS as a means to assess stability constants. The first arises from the restricted ionic conditions that can be investigated;[38] the use of sodium salts to maintain a constant (and high) ionic strength in the solutions was avoided, since it was observed to considerably alter the ESI-MS response. In fact, almost all earlier metal complexation studies by ESI-MS were conducted using solutions of low

5

ionic strength, without any addition of electrolyte.[39] The second difficulty comes from analysis of the gas-phase species coming from $Ln^{3+}(aq)$, the "free" Ln(III) in aqueous solution. A few authors provided some of the first examples of Ln(III) inorganic species observed by ESI-MS,[40] indicating that Ln(III) ions are strongly solvated in aqueous solutions (aquo ions $Ln(H_2O)_n^{3+}$ (n = 8-9)), and undergo gas-phase reduction in the transition from the condensed phase to the gas-phase leading to a variety of ionic species, bare metal ions (Ln^+ and/or Ln^{2+}), oxides, hydroxides, or Ln^{3+} clusters. It is noteworthy that, in aqueous solutions free of organic solvent, the ion intensity of Ln^{2+} becomes important for the lanthanides higher than La, Ce and Pr.[40b] It follows a quite low total ion intensity, due probably to a lower ion transmission efficiency of doubly-charged bare metal ion, when using a quadrupole mass spectrometer. By contrast, the lower mass lanthanides La, Ce and Pr, which are strong oxide formers, appear as oxide $[LnO(H_2O)_n]^+$ or hydroxide $[LnOH(H_2O)_n]^{2+}$ clusters in spectra, and the total ion intensity could be analytically useful for the determination of the initial aqueous concentrations.

In this study, we evaluated the use of nanoESI-MS as a means to obtain speciation information in sulfate/Ln(III) aqueous solutions. The nanoESI process is based on a capillary action induced by an applied electric field to draw the solution to the emitter tip.[41] The solution flow rates are about 100 times lower than those used with ESI (generally 10 μl per minute with a syringe pump). In addition to being more sensitive than conventional ESI, the spray is generated at lower temperature, voltage and flow rate, which are favorable conditions where the gas-phase ions are representative of the stability of the aqueous species. To our knowledge, this is the first report using a nanoESI-MS approach to determine the formation constant of a metal complex. Herein we focused on the monosulfate complex of La(III) formed in solutions at low ionic strength. Lanthanum was chosen rather than higher mass lanthanides, to avoid the formation of Ln^{2+} bare metal ions from the aqueous solutions and thereby to ensure analytically useful metal ion signals. Further investigations on Ln(III) sulfate complexes were carried out by using TRLIL. Europium was chosen to take advantage of its luminescence properties. Using TRLIL, the $EuSO_4^+$ and $Eu(SO_4)_2^-$ species were characterized for their formation constants, as well as their first coordination sphere environment through lifetime

6

measurements. A speciation model is proposed and formation constants were determined from the TRLIL data obtained in various ionic conditions. The Specific ion Interaction Theory (SIT) formula[9,42] was used for the description of the ionic medium/ionic strength dependence of the activities (effective concentrations) of the species involved in the equilibrium reactions. The value of the SIT coefficient $\varepsilon_{Eu^{3+},SO_4^{2-}}$ was reported as the first experimental estimation to our knowledge for a SIT coefficient between multi-charged species.

2. Experimental Section

Materials. Millipore deionized water (Alpha-Q, 18.2 MΩ cm) was used throughout the preparations. The lanthanide solutions were prepared from $La(NO_3)_3,6H_2O$ (Prolabo, Rectapur®, 99.99%) and Eu_2O_3 (Johnson Matthey, 99.99%). The perchloric, nitric and sulphuric acid concentrations were adjusted by using 1 M stock solutions prepared from $HClO_4$ 70% (Merck, GR for analysis), HNO_3 65% (Merck, Suprapur®) and H_2SO_4 98% (BDH, Aristar®), respectively, and all titrated with 0.1 M NaOH (Merck, Titrisol®). $NaClO_4,H_2O$ (R.P. Normapur™, >99.0%) and Na_2SO_4 (R.P. Normapur™, >99.5%) were purchased from Merck and used without further purification.

Preparation procedures. All the preparations and measurements were performed at (23±1)°C. NanoESI-MS measurements were performed in HNO_3/H_2SO_4 solutions of La(III). Nitric acid was used rather than perchloric acid which produced scattered MS signals due to isotopic effect of Cl. pH was measured using a combined glass electrode (XC161, Radiometer Analytical) that was calibrated for its linear response with commercial pH standards (Schott) with an estimated uncertainty of ±0.05. Since the ionic strength was low, typically 0.01-0.02 M, the effect of the junction potential was neglected. H^+ concentrations were deduced from the pH measurements that were corrected for the activity coefficient of H^+ calculated with the SIT formula (see Eq. 7). Two sets of experiments have been done at pH ~2 with 10^{-3} and 5×10^{-4} M $La(NO_3)_3$. Various volumes of a 0.01 M H_2SO_4 solution (pH = 1.83) were successively added to a 0.01 M HNO_3 solution (pH = 2.02), both with the same $La(NO_3)_3$ concentration, and pH was measured after each addition. Another set of experiments

7

was similarly performed by mixing 0.1 M HNO_3 and 0.1 M H_2SO_4 solutions, both with 10^{-3} M $La(NO_3)_3$. Since pH was out of the calibration range of the electrode, $[H^+]$ was calculated from the initial concentration of the acids, the mass action law for the HSO_4^- dissociation, and the mass conservation and electroneutrality relationships. $[H^+]$ was found to be close to 0.1 M when mixing together the two solutions. In each set, the ratio of nitric acid to sulphuric acid was varied in order to obtain increasing sulfate concentrations, while maintaining the ionic strength and pH roughly constant, so that the compositions of the working solutions were: $[SO_4^{2-}] = 10^{-4}$-5.6×10^{-3} M (1.83 < pH < 2.02) with the ionic strength, I, varying from 0.01 to 0.02 M, and $[SO_4^{2-}] = 10^{-3}$-2×10^{-2} M (0.100 < $[H^+]$ < 0.092 M) with I from 0.10 to 0.14 M.

For TRLIL measurements, all the aqueous solutions were prepared with 10^{-4} M Eu(III) to keep [Eu(III)] constant along the titrations. A first set of experiments was carried out at low ionic strength by titrating a 0.01 M $HClO_4$ solution with a 0.01 M H_2SO_4 solution, and pH was measured as for the similar titration series in 0.01 M HNO_3/H_2SO_4 solutions for nanoESI-MS measurements. Two other sets of experiments were carried out at higher ionic strengths and pH > 3: Titrations were performed using the initial Eu(III) solutions of 10^{-3} M $HClO_4$ at I = 0.50 and 2.00 M ($NaClO_4$), and 0.30 M Na_2SO_4 as the titrant solution (-log$[H^+]$ = 3.9, I = 0.90 M). The H^+ concentration of the Na_2SO_4 stock solution was determined by potentiometric measurements using an electrode whose reference compartment was filled up with a 0.99 M $NaClO_4$ / 0.01 M NaCl solution in order to minimize the effect of the junction potential, and which was calibrated for H^+ concentration with H^+ buffer solutions at I = 1 M. The ionic strength of the titrated solutions was calculated from the added volumes and was ranging between 0.50 and 0.70 M, and 1.45 and 2.00 M for each series. As no acido-basic reaction was expected during titration, $[H^+]$ was rather calculated and not measured in order to limit systematic errors in potentiometric measurements due to the small variations of I.

Time-Resolved Laser-Induced Luminescence. Details about our "FLUO 2001" experimental set-up have been given elsewhere.[43] The main features of the excitation source are briefly given here as it was different from that used in our previous studies. The excitation laser beam was generated by a

8

266 nm quadrupled Brilliant Nd-YAG laser, coupled to an optical parametric oscillator system (Quantel, France). The wavelength was tuned to 395 nm, providing about 2 mJ of energy in a 5 ns pulse with a repetition rate of 10 Hz. The data were treated using the OriginPro7 software (OriginLab™).

NanoElectrospray Ionization - Mass Spectrometry. The mass spectra were recorded in positive ion mode using a μ-Quattro triple-quadrupole spectrometer equipped with a nanoES interface (Micromass, Manchester, UK). A 20-μL emitter tip was filled up with the solution to be analyzed, and placed at 3 mm from the inlet orifice to the mass spectrometer (the optimal location that maximizes the signal response); a voltage of 1.5 kV was supplied to the emitter tip to conduct nanoelectrospray, providing a flow rate which has been determined to be about 0.1 μL/min. The emitter tip was repositioned at its optimal location for each repeated analysis. The source temperature was set to 80°C, and the sample cone voltage was set within the range 20-50 V. Spectra were acquired at 6 s/scan over a mass range of m/z 50-1200 with an acquisition time of 3 min. For MS/MS measurements, collision-induced dissociation of cluster ions was performed with argon; the collision gas pressure was 2×10^{-3} mbar. Spectra were obtained at different collision energies ranging from 5 to 30 eV.

3. Results and discussion

Thermodynamic equations. The stepwise formation constants for the monosulfate and disulfate complexes of M^{3+} f-element are

$$\beta_1 = \frac{[MSO_4^+]}{[M^{3+}][SO_4^{2-}]} \tag{Eq. 1}$$

$$K_2 = \frac{[M(SO_4)_2^-]}{[MSO_4^+][SO_4^{2-}]} \tag{Eq. 2}$$

respectively. The stability of $M(SO_4)_2^-$ complex is equivalently defined by the overall stability

constant $\beta_2 = \beta_1 K_2$. The formation constants extrapolated to zero ionic strength, $K°$, were calculated with the SIT formula:

$$\log K° = \log K_m - \Delta z^2 D + \Sigma_{i,j} \, \varepsilon_{i,j} \, m_j \qquad \text{(Eq. 3)}$$

where the subscript m denotes the molality scale, and K_m is related to K through molal-to-molar conversion factors.[42] $D = 0.509 I_m^{1/2}/(1 + 1.5 I_m^{1/2})$ is the Debye-Hückel term, I_m is the ionic strength (mol kg^{-1}), Δz^2 is calculated from the charges of the species of the corresponding equilibrium: The values are typically -12, -4 and -16 for β_1, K_2 and β_2, respectively. $\varepsilon_{i,j}$ is an empirical ion pair interaction coefficient for the pair of species i and j; $\varepsilon_{i,j}$ is assumed to equal zero for ions of same charge-sign. Numerical values of $\varepsilon_{i,j}$ were taken from the literature (Table 2) when available, or obtained as explained below. m_j is the molal concentration of the species j. The concentration of the free SO_4^{2-} ligand was calculated with Eq. 4 when the concentrations of Ln(III) sulfate complexes were negligible in the mass balance of sulfate, that is for the Eu(III) experiments, where the effect of metal complexation on $[SO_4^{2-}]$ was finally calculated to be less than 0.5%:

$$[SO_4^{2-}] = \frac{[SO_4]_0}{1 + K_b [H^+]} \qquad \text{(Eq. 4)}$$

where $[SO_4]_0$ is the total sulfate concentration.

$$K_b = \frac{[HSO_4^-]}{[SO_4^{2-}][H^+]} \qquad \text{(Eq. 5)}$$

is the basicity constant, and was calculated for each studied ionic medium using the SIT formula and the appropriate $\varepsilon_{i,j}$ coefficients (Table 2). For La(III) experiments, sulfate complexation was accounted for in the mass balance leading to Eq. 9 (see below). The dependence of K_b with the ionic strength had already been proposed by Grenthe et al. on the basis of four sets of experimental values in solutions with NaClO$_4$ as a supporting electrolyte;[44] in this case Eq. 3 simplifies as,

$$\log K_{b,m} = \log K_b° - 4 D - \Delta\varepsilon \, m_{NaClO_4} \qquad \text{(Eq. 6)}$$

which was found to be reliable (Figure 1), and resulted in $\log K_b° = 1.98_9 \pm 0.08_4$ and $\Delta\varepsilon = (0.00_3 \pm 0.05_1)$ kg mol^{-1}. In our work some of the solutions contained significant amounts of Na$_2$SO$_4$ salt, so that the simplified SIT formula (Eq. 6) was not well adapted. The SIT term was thus developed to account for interactions with the main ions in the solutions, $i.e.$ Na$^+$, ClO$_4^-$ and SO$_4^{2-}$ for -log[H$^+$] > 3. The corrected $\log K_{b,m}$ values slightly deviated from those in a pure NaClO$_4$ medium when SO$_4^{2-}$ was not negligible against ClO$_4^-$, and for $I_m > 0.5$ mol kg^{-1} (Figure 1). Conversely, this correction was found to be negligible for the HClO$_4$/H$_2$SO$_4$ and HNO$_3$/H$_2$SO$_4$ working solutions for which $I_m < 0.1$ mol kg^{-1} and -log[H$^+$] > 1. Figure 1 also illustrates the case of H$_2$SO$_4$ solutions without any supporting electrolyte: The calculated values deviate from the case with NaClO$_4$ only when $I_m > 0.3$ mol kg^{-1}, $i.e.$ when -log[H$^+$] < 0.5. In this case, the SIT term, $\Sigma_{i,j}\ \varepsilon_{i,j}\ m_j$ (Eq. 3), had a much smaller effect on $\log K_{b,m}$ values than the Debye-Hückel contribution, Δz^2 D. For the experiments at pH lower than 2 and low ionic strength, a more significant effect originated from the determination of the ligand concentrations from pH measurements according to Eq. 4. Indeed, when pH was measured instead of -log[H$^+$], K_b was corrected for γ_{H^+}, the activity coefficient of H$^+$ calculated as

$$\log \gamma_{H^+} = \text{-D} + \varepsilon_{H^+,ClO_4^-}\ m_{ClO_4^-} + \varepsilon_{H^+,NO_3^-}\ m_{NO_3^-} + \varepsilon_{H^+,HSO_4^-}\ m_{HSO_4^-} + \varepsilon_{H^+,SO_4^{2-}}\ m_{SO_4^{2-}} \qquad \text{(Eq. 7)}$$

We evaluated the unknown value of $\varepsilon_{H^+,HSO_4^-}$ by correlating available ε_{M^+,X^-} values with ε_{Na^+,X^-} published ones[42] or calculated from the well-known corresponding Pitzer coefficients,[45] we obtained $\varepsilon_{H^+,HSO_4^-} = \varepsilon_{Na^+,HSO_4^-} + (0.11 \pm 0.05)$. The H$^+$ activity correction on $\log K_b$ ranged from 0.04 to 0.06, hence from 0.02 to 0.03 on $\log[SO_4^{2-}]$.

ESI-MS results for La(III). Ln(III) complexes are usually classified as kinetically labile on the basis of fast formation and dissociation rate constants that reflect the strong ionic nature of f-element bonding. The kinetics of LnSO$_4^+$ complexes has been examined by sound absorption techniques from which stability constants were obtained for La and Eu (Table 1);[18,25] these studies have shown high rate constants for the formation of an inner sphere complex from the outer sphere complex (k_f

1.0-3.4×10^8 s^{-1}), as well as for its dissociation (k_d 2-7×10^7 s^{-1}). Nevertheless, there is increasing acceptance that speciation of kinetically labile species can be maintained on the time scale of the ESI process; for instance reliable formation constants were reported for metal complexes with k_f ~10^5-10^9 s^{-1}.[46] In previous studies, it has been shown that formation constants of lanthanide and actinide complexes can be directly determined from quantitation of total metal speciation achieved by monitoring gas-phase species coming from all free and complexed aqueous species.[36,37] This procedure was also used in the present study. The positive ion mode was required for the detection of positively-charged ions induced by La^{3+}(aq) and LaSO$_4^+$(aq). La(SO$_4$)$_2^-$(aq) was however likely to produce negatively-charged ions, for which a negative ion mode was required. Simultaneous detection of positive and negative gas-phase ions is not possible; consequently it is also not possible to make any direct comparison of the intensities measured in the two detection modes. For this reason, experimental conditions were chosen so as to preferentially form La^{3+}(aq) and LaSO$_4^+$(aq) with negligible concentrations of the disulfate complex. Nevertheless, this latter species was formed at higher sulfate concentrations obtained by increasing the H$_2$SO$_4$ concentration and thereby decreasing the pH from about 2 to 1. The species identified in the nanoESI-MS spectra are summarized in Table 3. MS/MS experiments involving collision-induced dissociation (CID) have been used to probe the molecular ions generated by nanoESI (Table S1, Supporting Information). The assignments reported in Table 3 agree with the detected daughter ions observed in representative MS/MS spectra and the corresponding mass loss.

Quantitation of total La(III) speciation was achieved under relatively mild ion-source energy (ion cluster mode). Figure 2 shows a representative nanoESI mass spectrum obtained in the positive ion mode for an aqueous solution containing 10^{-3} M La(NO$_3$)$_3$ and a 2-fold molar ratio of SO$_4^{2-}$ at pH 2. Whereas the [La(H$_2$O)$_9$]$^{3+}$(aq) ion is known to be the predominant species in the aqueous phase at pH 2, it was detected in spectra as oxides, hydroxides, and La^{3+} clusters (Table 3). The hydroxide ions [LaOH(H$_2$O)$_n$]$^{2+}$ and oxide ions [LaO(H$_2$O)$_n$]$^+$ were observed. MS/MS spectrum confirmed the assignments, where the loss of water molecules from the solvation shell is the major fragmentation pathway for these ions (Table S1). The oxide ions are the predominant species throughout the

spectra. One can also observe that the high nitrate content of the solutions promotes the formation of oxide ions that retain HNO_3 during the gas-phase ion formation, such as $[LaO(H_2O)(HNO_3)]^+$ and $[LaO(HNO_3)]^+$. The likely species $[La(NO_3)_2(H_2O)_n]^+$ that involve nitrate anions have also been identified by MS/MS experiments. For instance, MS/MS spectra of the $[La(NO_3)_2(H_2O)]^+$ ion shows that this ion readily lost H_2O or decomposed under higher energetic conditions to give an oxide ion $[LaO(HNO_3)]^+$. The analysis of these species to evaluate La(III) complexation by nitrate is not straightforward. Because nitrate complexation is not very strong (log β_1 slightly more than 1), the association of the La^{3+} analyte ion with the not very volatile NO_3^- ligand may occur either in the aqueous solution, or during the solution-to-gas phase transition leading to a non-specific binding (cluster formation). The molar fraction of the $LaNO_3^{2+}$(aq) species in the aqueous solution was therefore calculated. Generally, f-elements are not expected to form aqueous complexes with perchlorate anions, while inner sphere nitrato complexes have been proposed.[47] Hence, complexation by nitrate should be accounted for. This was determined from thermodynamic calculations using data for the analog Am(III): log $\beta_1°$($AmNO_3^{2+}$) = $1.3_3\pm0.20$.[10] The contribution of $LaNO_3^{2+}$(aq) in La(III) speciation was found to be less than 14% and 6% for pH 1 and 2, respectively. As indicated below, this contribution has been taken into consideration in the analysis of the MS data. The weak influence of nitrate complexes at pH 2 was also supported by the TRLIL results for equivalent HNO_3/H_2SO_4 solutions of Eu(III): The luminescence spectra did not significantly differ from those for $HClO_4/H_2SO_4$ solutions.

Concerning the monosulfate complex, $LaSO_4^+$(aq), the ions observed in the mass spectra correspond to $[La(SO_4)(H_2O)_n]^+$, as well as mixed-solvent clusters, $[La(SO_4)(H_2O)_n(HNO_3)]^+$ and $[La(SO_4)(H_2O)_n(H_2SO_4)_m]^+$. The effect of the non-specific binding of SO_4^{2-} during the ES desolvation process should be smaller than the complexation in the aqueous solution and was thereby neglected. MS/MS spectra evidenced that these species dissociate by loosing solvent molecules that surround the $LaSO_4^+$ ion (Table S1). Furthermore, it was found that under high energetic conditions, fragmentation of the $[La(SO_4)(H_2O)_2]^+$ and $[La(SO_4)(H_2O)_2(HNO_3)]^+$ complexes leads to the $[LaO(H_2O)]^+$ and $[LaO(HNO_3)]^+$ oxide species, respectively.

The efficiency of the conversion to ions in the gas-phase is likely to be similar for the various species, as already observed from ion intensity measurements.[38] The detection yields are also likely to be similar for the monocharged gas-phase ions in the 120-500 m/z range. Consequently, the summation of the ionic currents of the gas-phase species (Table 3) were assumed to be proportional to the aqueous concentrations of either the free ion or the monosulfate complex. The ratio $R = [LaSO_4^+(aq)]/[La^{3+}(aq)]$ was thereby calculated after $[La^{3+}(aq)]$ was corrected for the weak nitrate complexation by subtracting the calculated concentration of $LaNO_3^{2+}(aq)$, which only slightly increased the R values. The equilibrium constant β_1 was determined from the mass action law

$$\log R = \log \beta_1 + \log[SO_4^{2-}]$$
(Eq. 8)

and the equilibrium concentration of $SO_4^{2-}(aq)$

$$[SO_4^{2-}] = \frac{[SO_4]_0 - [La]_0\left(\dfrac{R}{R+1}\right)}{1 + K_b[H^+]}$$
(Eq. 9)

For 10^{-3} M and 5×10^{-4} M La(III) solutions, plotting log R vs log[SO_4^{2-}] gave a straight line of slope +1 and intercept log β_1 according to Eq. 8 (Figure 3). The slope +1 reflects the 1-1 stoichiometry of the aqueous complex, which is good indication that we made reasonable assumptions for the quantitative interpretation of MS data. For twice-diluted La(III) solutions at 5×10^{-4} M, whereas two of the dots were consistent with the model, two others significantly deviated, which was attributed to very low ion intensities close to the detection limits, thus influencing the determination of R. In a few solutions with the highest [SO_4^{2-}], the formation of $La(SO_4)_2^-(aq)$ was suspected, and actually detected by using the negative ion mode (Fig. S1, Table S2). Since the consumption of SO_4^{2-} due to the formation of $La(SO_4)_2^-(aq)$ was neglected in Eq. 9 because it could not be properly calculated, the corresponding experimental dots were expected to deviate from the model towards elevated [SO_4^{2-}] as observed for [SO_4^{2-}] > 0.01 M. This effect was even more stressed than expected, possibly due to higher uncertainties on [$La^{3+}(aq)$] that was determined from the peaks of low ion intensities; the $La^{3+}(aq)$ concentration actually became lower than about 13% of the total lanthanum

concentration under these conditions.

Linear regression analysis of the nanoESI-MS data provided intercepts 3.0±0.2 and 2.9±0.3 for pH 1 and 2, respectively (±1.96×σ, where σ is the standard deviation). Correction for nitrate complexation was only significant for pH 1: log β_1 = 3.1±0.3 (Figure 3). A good agreement between the log β_1 values was observed within uncertainties although a slight difference should be expected due to the difference of ionic strengths. The log β_1 values were extrapolated to $I = 0$ using the simplified SIT formula

$$\log \beta_1^\circ = \log \beta_{1,m} + 12\,D + \Delta\varepsilon\,I_m \qquad\qquad\qquad \text{(Eq. 10)}$$

as the influence of the ion pair term ($\Delta\varepsilon\,I_m$) was small for $I < 0.1$ M. This term associated to the complexation reaction was taken as: $(\varepsilon_{LaSO_4^+,HSO_4^-} - \varepsilon_{La^{3+},HSO_4^-})\,m_{HSO_4^-} - \varepsilon_{H^+,SO_4^{2-}}\,m_{H^+} \approx -0.0_6\pm0.1_7$ (Table 2). This definition is consistent with a predominance of HSO_4^-, which is a rough approximation because, beside HSO_4^-, the solutions also contained the NO_3^- and SO_4^{2-} counter-anions. However, the assumption was found to be relevant since the $|\Delta\varepsilon\,I_m|$ term was calculated to be always less than 0.03, and did not significantly influence the calculations. Ionic strength corrections, log β_1° - log $\beta_{1,m}$, were calculated from Eq. 10 and were found to equal 1.32±0.03 and 0.60±0.01 for $I = 0.1$ and 0.01 M, respectively, which corresponds to pH 1 and 2, respectively. Hence, log β_1° was calculated as 4.4±0.3 and 3.5±0.3 from the two series of experiments. The too high log β_1° value of 4.4±0.3 compared to other data (Table 1) was thought to result from non-specific binding during the ESI desolvation process, since the sulfate concentrations in solutions at pH 1 were higher than those in the solutions at pH 2. The value determined by nanoESI-MS from dilute solutions at pH 2 is presented with other published values for La(III) in Table 1. Direct comparison is only possible for the data extrapolated to $I = 0$ for which the agreement is good. The values obtained by different workers from conductimetry are about 3.6 while a calorimetric study provided 3.5. Another value reported in a potentiometric study, is about 0.3 log unit higher than the nanoESI-MS value. The uncertainty of ±0.3 is larger than those previously proposed from other techniques (Table 1). This is mainly due to the difficulty of making quantitative measurements for the free La(III) in aqueous

solutions without organic solvents. However, the quantitative agreement demonstrates the potential of nanoESI-MS for kinetically labile species. Within its uncertainty, the MS value of 3.5±0.3 lies between the data selected by Silva *et al.* (3.85±0.03) for Am(III)[9] and the one (3.30±0.15) for Cm(III),[10] and cannot really help to discuss these values.

TRLIL results for Eu(III). The evolution of TRLIL spectrum is presented in Figure 4 for increasing sulfate concentrations ($[SO_4^{2-}]$ = 0-0.2 M in Na_2SO_4/$NaClO_4$ aqueous media at I = 0.50-0.70 M and $3 < -\log[H^+] < 3.9$). Spectroscopic features of uncomplexed Eu(III) in aqueous perchlorate medium have been emphasized in extensive studies of solution chemistry of europium.[32a,48] The TRLIL spectra obtained with solutions of Eu^{3+} in the presence of only perchlorate anions present four characteristic bands centred at 593, 618, 650 and 700 nm corresponding to radiative transitions from the $^5D_0$ excited state to the $^7F_1$, $^7F_2$, $^7F_3$ and $^7F_4$ ground state manifold, respectively. The strongest transitions are $^5D_0 \rightarrow {}^7F_{1,2,4}$ while $^5D_0 \rightarrow {}^7F_3$ is weaker because it is forbidden according to Laporte's selection rules. The $^5D_0 \rightarrow {}^7F_2$ transition (electric dipole) exhibits hypersensitivity and can be used as a luminescence probe for complexation analyses; its intensity increases much more than those of other transitions upon complexation. Interestingly, the non-degenerated $^5D_0 \rightarrow {}^7F_0$ transition at 580 nm only occurs when the local symmetry of Eu^{3+} is low, particularly when there is no inversion center, so it evidences inner sphere complex formation.

While increasing the sulfate concentration, the hypersensitive transition peak at 618 nm changed more significantly in intensity and position than other peaks (Figure 4); a slight shift (about 2 nm) of its maximum towards the low wavelengths was observed. These spectral changes were attributed to the formation of the sulfate complexes of Eu(III). The enhancements of the peaks at 593 and 700 nm likely indicate that at least one of the Eu(III) species has either a higher luminescence quantum yield or a higher absorption coefficient than Eu^{3+} at the 395 nm excitation wavelength. The detection of the $^5D_0 \rightarrow {}^7F_0$ emission at 580 nm is consistent with complex formation.

16

The quantitative analysis of TRLIL spectra was based on the intensity changes of the hypersensitive transition peak. The measured intensity, I_{mes}, was normalized (I_{norm}^R) in relation to $[Eu]_T$, the total europium concentration, and I_0°, the molar fluorescence intensity of Eu^{3+}. As for classical spectrophotometry, the change of the Eu(III) emission was described with the theoretical expression:

$$I_{norm}^R = \frac{I_{mes}}{[Eu]_T I_0^\circ} = \frac{\sum_{0<i<2}(I_i^R \, \beta_i [SO_4^{2-}]^i)}{\sum_{0<i<2}(\beta_i [SO_4^{2-}]^i)} \tag{Eq. 12}$$

where $I_i^R = I_i^\circ / I_0^\circ$ and I_i° is the molar fluorescence intensity of $Eu(SO_4)_i^{3-2i}$. According to the SIT formula, the dependences of the formation constants with the ionic strength are

$$\log \beta_{1,m} = \log \beta_1^\circ - 12\,D - \Delta_1(\varepsilon m) \tag{Eq. 13}$$

$$\log K_{2,m} = \log K_2^\circ - 4\,D - \Delta_2(\varepsilon m) \tag{Eq. 14}$$

The SIT terms, $\Delta_1(\varepsilon m)$ and $\Delta_2(\varepsilon m)$, are related to the interactions with the ionic components of the solutions.[49] Some of the ε values involved in $\Delta_1(\varepsilon m)$ and $\Delta_2(\varepsilon m)$ were available in the literature or estimated by analogy to other M^{3+} cations, while $\varepsilon_{Eu^{3+},HSO_4^-}$, $\varepsilon_{Eu^{3+},SO_4^{2-}}$, $\varepsilon_{EuSO_4^+,HSO_4^-}$, $\varepsilon_{EuSO_4^+,SO_4^{2-}}$ and $\varepsilon_{H^+,Eu(SO_4)_2^-}$ were unknown (Table 2). The determination of these latter parameters by curve fitting technique turned out to be not relevant since their influence on ionic strength corrections was not so high compared to a mean $\Delta\varepsilon$ value in a simplified SIT formula. Hence, we found it better to estimate them using correlations as already proposed.[44,50] For a given anion X^-, ε_{M^{z+},X^-} were found to correlate linearly with $z/r_{M^{z+}}$ where $r_{M^{z+}}$ is the ionic radius of M^{z+}.[51] Hence to determine $\varepsilon_{Eu^{3+},HSO_4^-}$, we calculated $\varepsilon_{K^+,HSO_4^-}$, $\varepsilon_{Mg^{2+},HSO_4^-}$, $\varepsilon_{Ca^{2+},HSO_4^-}$ and $\varepsilon_{Fe^{2+},HSO_4^-}$, from Pitzer parameters for the corresponding interactions.[45] The linear regression applied to these four values and the tabulated $\varepsilon_{Na^+,HSO_4^-}$[42] gave: $\varepsilon_{M^{z+},HSO_4^-} = 0.186\,(z/r_{M^{z+}}) - 0.196$ ($R^2 = 0.93$). We also obtained $\varepsilon_{MSO_4^+,SO_4^{2-}} = 0.205\,(z/r_{M^{z+}}) - 0.331$, but using only the two tabulated values for $\varepsilon_{Li^+,SO_4^{2-}}$ and $\varepsilon_{Na^+,SO_4^{2-}}$.[42] We estimated the value of $\varepsilon_{EuSO_4^+,HSO_4^-}$ as $(\varepsilon_{AmSO_4^+,ClO_4^-} + \varepsilon_{Na^+,HSO_4^-} - \varepsilon_{Na^+,ClO_4^-}) = 0.2_0 \pm 0.1_0$ from

tabulated data.[42] This estimation is consistent with what would be found by Ciavatta's method:[52] $\varepsilon_{EuSO_4^+,HSO_4^-} \approx (\varepsilon_{Eu^{3+},HSO_4^-} + \varepsilon_{Na^+,SO_4^{2-}})/2 = 0.1_1 \pm 0.1_5$. $\varepsilon_{H^+,Eu(SO_4)_2^-}$ was not determined because of its negligible effect under our conditions. Hence $\varepsilon_{Eu^{3+},SO_4^{2-}}$ was the only fitted specific ion coefficient as it involves multi-charged species for which correlations are not obvious, although it only had a weak influence on the fit for $[SO_4^{2-}] > 0.1$ M.

The luminescence spectra have been obtained for three series of titration experiments in different ionic conditions: 0.02-0.05 M H^+ (H_2SO_4/$HClO_4$), 0.40-0.55 M Na^+ and 2.00-1.30 M Na^+ (Na_2SO_4/$NaClO_4$). The intensities I_{norm}^R at 618 nm are plotted against $\log[SO_4^{2-}]$ in Figure 5. The sensitivity of the analysis was assessed by examining several curve fits, where $\log \beta_1$ and $\log K_2$ were taken as functions of ionic media using Eqs. 13 and 14. The three more significant modelings are represented in Figure 5(a). The aim was to determine the speciation model that best described the data. When assuming the formation of $EuSO_4^+$ only, *i.e.* adjusting $\log \beta_1^\circ$ and I_1^R, the modeling deviated from the data, except when $\log[SO_4^{2-}] < -2.8$ for the series with low ionic strength (Model A). A better fit, very similar to Model B, was obtained when also adjusting $\varepsilon_{Eu^{3+},SO_4^{2-}}$ that took the value 6.9; this very high value is however unrealistic and only reflects the correlation between ε parameters and stability constants. Model B was based on the assumption that $EuSO_4^+$ and $Eu(SO_4)_2^-$ formed, and that both complexes had the same I°, which could be the case for instance if the second SO_4^{2-} do not enter into the first coordination sphere of Eu^{3+}, but rather forms an outer sphere complex, $EuSO_4^+,SO_4^{2-}$. Details of the calculations are given in Appendix. The corresponding fitted curves described fairly well the data; for the lowest ionic strength series, the few data dots at $\log[SO_4^{2-}] > -2.6$ fell down the curve, whereas for the other two series, the curvature was too high to perfectly match the data for $-3 < \log[SO_4^{2-}] < -1.7$. In Model C, $\log \beta_1^\circ$, $\log K_2^\circ$, I_1^R and I_2^R were fitted, and the resulting curves better described the three sets of experiments. Model C was thus found to be more relevant suggesting that $EuSO_4^+$ and $Eu(SO_4)_2^-$ formed, each species defined by a specific I^R value. The fit with Model C finally resulted in $\log \beta_1^\circ = 3.7_8 \pm 0.1$ and $\log K_2^\circ = 1.5 \pm 0.2$, and the relative intensities at 618 nm, $I_1^R = 2.6 \pm 0.1$ and $I_2^R = 5.6 \pm 0.3$. A possible further complex

$Eu(SO_4)_3^{3-}$ was insignificant under these conditions. The speciation diagrams are presented in Figure 5(b) for the three sets of ionic conditions. As expected, $EuSO_4^+$ was the major species (> 70%) at low ionic strength ($I = 0.02$ M) in relation to the Eu^{3+} aquo ion that was better stabilized at higher I. The formation of $Eu(SO_4)_2^-$ was observed when increasing the sulfate concentration and was even the major complex (~60%) at medium ionic strength ($I = 0.55$ M).

The formation constants are reported in Table 1 with other published values for Eu(III). The values at zero ionic strength show a good agreement between our TRLIL data and the ones obtained by other techniques such as sound absorption, electrophoresis and solvent extraction, despite the scattering of the log K_2 values from the literature for a given ionic strength. Interestingly, our results also agree well with the data for Am(III) and Cm(III) obtained by solution-based methods,[9] but are significantly higher than those for Cm(III) obtained by TRLIL.[33,34] No explanation can be reasonably offered for this latter observation, except that the studies were carried out in different ionic media (NaClO$_4$ vs NaCl). This however should not be responsible of such differences, unless medium effects favored ion pairing, which is unlikely. Figure 6 illustrates the ionic strength dependence of β_1 up to 2 M for a NaClO$_4$ medium. The nanoESI-MS and TRLIL log β_1 values as well as published data for the La(III) and Eu(III) are consistent with the SIT formula for a NaClO$_4$ electrolyte. Some of our experimental values deviate because we accounted for short-range interactions with SO_4^{2-} as in the calculation of K_b. Thus, these data were naturally closer to the SIT curve corresponding to a pure Na$_2$SO$_4$ medium. The fitted value of $\varepsilon_{Eu^{3+},SO_4^{2-}}$ was found to be $0.8_6\pm0.5$, and was associated with a large uncertainty, since it only influenced the data for $\log[SO_4^{2-}] > -1$. Anyhow, we obtained the first estimation to our knowledge for a SIT coefficient between multi-charged species.

The specific luminescence spectra for Eu^{3+}, $EuSO_4^+$ and $Eu(SO_4)_2^-$ were determined by spectral decomposition (Figure 7). The hypersensitive peak increases when the ligand binds Eu^{3+}, with slight differences of its shape in relation to different splitting effects of the $^7F_2$ level. For $EuSO_4^+$, the peaks at 593 and 700 nm are similar to that for Eu^{3+}, suggesting that the yield of the radiative deexcitation processes is the same, whereas the overall emission for $Eu(SO_4)_2^-$ is more intense, which is likely due to better absorption at 395 nm. As already noted, the detection of fluorescence at 580 nm

reveals changes of the symmetry of the hydrated Eu(III) indicating the replacement of one or more water molecules with one or two sulfate ions in the primary coordination sphere. The $EuSO_4^+$ and $Eu(SO_4)_2^-$ species were characterized for their first coordination sphere environment through lifetime measurements. As previously demonstrated, it is possible to correlate the primary hydration number of europium (N_{H_2O}) and the lifetime of its $^5D_0$ emitting level (τ).[53] Such a correlation was reported by Kimura and Choppin, $N_{H_2O} = 1070/\tau - 0.62$, providing hydration numbers with an uncertainty of ± 0.5.[54] Indeed, the lifetime measured for Eu(III) in a 0.01 M $HClO_4$ solution is 110 ± 10 µs which indicates the presence of nine water molecules in the internal coordination sphere of the Eu^{3+} aquo ion, while a hydration number between 8 and 9 is expected.[55] In all the solutions, the emission decay was treated with a single exponential curve. The corresponding lifetimes slowly increased with the formation of the mono and disulfate complexes. Hydration numbers were calculated from several lifetime measurements (Table 4), and were interpreted as averages of the hydration numbers of Eu^{3+}, $EuSO_4^+$ and $Eu(SO_4)_2^-$ weighted by their concentrations in the solution. These hydration numbers indicate the number of water molecules replaced by SO_4^{2-} for each species. When the monosulfate complex is predominant (0.01 M H_2SO_4 solution where metal speciation is: 19.4% Eu^{3+}, 74.0% $EuSO_4^+$, and 6.6% $Eu(SO_4)_2^-$), τ was measured to be 123 ± 10 µs, *i.e.* 8.1 ± 0.5 remaining water molecules. While increasing sulfate concentration up to 0.3 M, the predominant species is the disulfate complex (0.3 M Na_2SO_4 solution where metal speciation is: 7.9% Eu^{3+}, 36.8% $EuSO_4^+$, and 55.3% $Eu(SO_4)_2^{2-}$) and τ was 133 ± 10 µs, *i.e.* 7.4 ± 0.5 remaining water molecules. Considering different possible hydration numbers for each species, the most reliable set of values was found to be 9, 8 and 7 for Eu^{3+}, $EuSO_4^+$ and $Eu(SO_4)_2^-$, respectively, according to the speciation results. This is consistent with a mechanism where each sulfate molecule entering the internal coordination sphere of europium is likely to exclude one water molecule from the primary hydration sphere, suggesting that the sulfate ion acts as a monodentate ligand in aqueous solution. The same conclusion was previously made from sound absorption measurements.[25,56] The SO_4^{2-} substitution rates with lanthanides reported from these measurements are about $10^8 - 10^7$ s^{-1}; since these values are close to those found for water exchange, they have been interpreted as being indicative of the monodentate

nature of SO_4^{2-} binding. For instance, the exchange rates of acetate (CH_3COO^-) substitution are two orders of magnitude slower and were taken to be characteristic of a bidentate interaction.

The ratio of inner to outer sphere monosulfate complexes of lanthanides and actinides has been previously examined.[23,27] It is noteworthy that the interpretation of the luminescence spectra obtained in this study does not exclude the formation of outer sphere complexes. Several authors have discussed differences of stability constants of lanthanide complexes determined by spectrophotometric and solution-based methods, and concluded that only the formation constant of inner sphere complexes could be measured by spectrophotometric techniques.[10,26] This belief was found to be not consistent with thermodynamics, when equilibrium is achieved between inner and outer sphere complexes.[8] Despite spectroscopic changes are essentially due to inner sphere complexes, the actually measured formation constant is the sum of the formation constants for the inner and outer sphere species, $\beta^{(tot)} = \beta^{(in)} + \beta^{(out)}$, due to the equilibrium between the two complexes (see Appendix). This conclusion was also confirmed by Hale and Spedding from their UV absorption study dealing with the formation of $EuSO_4^+$.[27] For instance, DeCarvalho and Choppin have determined the formation constant of $EuSO_4^+$ in 2 M $NaClO_4$ solutions by potentiometry (log $\beta_1 = 1.37\pm0.08$) and solvent extraction techniques (log $\beta_1 = 1.38\pm0.06$);[23] these values are in good agreement with our TRLIL value at the same ionic strength (log $\beta_1 = 1.3_6\pm0.1$).

Conclusion

Sulfate complexation of La(III) and Eu(III) has been investigated for the first time to our knowledge by nanoElectrospray Ionization - Mass Spectrometry and Time-Resolved Laser-Induced Luminescence. From the interpretation of luminescence lifetimes, the sulfate anion was concluded to exchange with a single water molecule of the first coordination sphere, suggesting it is a monodentate ligand towards trivalent f-element cations. NanoESI-MS provided a relevant stability constant for the labile $LaSO_4^+$ complex, and confirmed its capacity to be a useful speciation tool for studies of inorganic aqueous speciation of metal ions. However, we could only use this technique for the characterization of species which were formed at low ionic strength. Stabilities of $EuSO_4^+$ and

$Eu(SO_4)_2^-$ were determined as functions of the ionic media by TRLIL. Our speciation model for Eu(III) was consistent with earlier investigations by classical techniques and, interestingly, with studies on Am(III) and Cm(III), suggesting a good analogy. This experimentally confirmed that spectroscopic techniques do not provide stability constants for only inner sphere complexes, but rather global constants for inner and outer sphere complexes, when existing. In equilibrium conditions in interstitial waters of clayey materials of the Callovo-Oxfordian clay formation, the ionic strength and the sulfate concentration had been estimated to be 0.1 M and 0.031 M, respectively. Under these conditions, the concentration ratios of $LnSO_4^+$ and $Ln(SO_4)_2^-$ over Ln^{3+} were calculated to be 10.3 and 3.9, respectively, using the stability constants determined in this work for Eu(III).

Acknowledgements

Appendix

The reaction of a ligand L^{y-} with an aquatic metal ion M^{z+} is generally described by the Eigen-Tamm mechanism,[57] whereby the ultimate step is an equilibrium between inner ($M_iL_j^{iz-jy\ (in)}$) and outer sphere ($M_iL_j^{iz-jy\ (out)}$) complexes as illustrated by Eq. A1 where δn denotes the hydration number variation.

$$M_iL_j^{iz-jy\ (in)} \rightleftharpoons M_iL_j^{iz-jy\ (out)} + \delta n\ H_2O \qquad \text{(Eq. A1)}$$

The thermodynamic constant that characterizes this equilibrium is:

$$k_{i,j} = \beta_{i,j}^{(out)} / \beta_{i,j}^{(in)} \qquad \text{(Eq. A2)}$$

where $\beta_{i,j}^{(in)}$ and $\beta_{i,j}^{(out)}$ are the formation constants of the inner and outer sphere complexes, respectively. Thus, the measured intensity, I_{mes} (light absorption or emission), writes

$$I_{mes} = \Sigma_{i,j}\ (I_{i,j}^{o(in)}\ [M_iL_j^{iz-jy\ (in)}] + I_{i,j}^{o(out)}\ [M_iL_j^{iz-jy\ (out)}] \qquad \text{(Eq. A3)}$$

where $I_{i,j}^{o(in)}$ and $I_{i,j}^{o(out)}$ are molar absorption coefficients or luminescence quantum yields. Eq. A3

also writes

$$I_{mes} = \Sigma_{i,j} (\beta_{i,j}^{(tot)} I_{i,j}^{\circ(tot)} [M^{z+}]^i [L^{y-}]^j)$$ (Eq. A4)

where we have noted

$$\beta_{i,j}^{(tot)} = \frac{[M_iL_j^{iz-jy\,(in)}] + [M_iL_j^{iz-jy\,(out)}]}{[M^{z+}]^i[L^{y-}]^j} = \beta_{i,j}^{(in)} + \beta_{i,j}^{(out)}$$ (Eq. A5)

$$I_{i,j}^{\circ(tot)} = \frac{\beta_{i,j}^{(in)} I_{i,j}^{\circ(in)}}{\beta_{i,j}^{(tot)}} + \frac{\beta_{i,j}^{(out)} I_{i,j}^{\circ(out)}}{\beta_{i,j}^{(tot)}} = \frac{I_{i,j}^{\circ(in)}}{1 + k_{i,j}} + \frac{I_{i,j}^{\circ(out)}}{1 + \dfrac{1}{k_{i,j}}}$$ (Eq. A6)

which demonstrates that the formation constant measured for a species $M_iL_j^{iz-jy}$ is actually the sum of the formation constants for the inner and outer sphere species. The $M_iL_j^{iz-jy}$ species is thus characterized by $I_{i,j}^{\circ(tot)}$ and $\beta_{i,j}^{(tot)}$, and not by $I_{i,j}^{\circ(in)}$ and $\beta_{i,j}^{(in)}$. In this work, mono-nuclear species of M^{3+} are involved (i = 1 and is omitted), and Eq. A4 results in an equation similar to that used for the TRLIL data analysis (Eq. 12):

$$\frac{I_{mes}}{[M]_T} = \frac{\sum_{0<j<2}(I_j^{\circ(tot)} \beta_j^{(tot)}[L^{y-}]^j)}{\sum_{0<j<2}(\beta_j^{(tot)}[L^{y-}]^j)}$$ (Eq. A7)

Even if spectral changes usually originate from the formation of inner sphere complexes, the measured intensity probes the formation of both inner and outer sphere complexes, whose ratio is actually constant, and equal to $k_{i,j}$ (Eq. A2). For instance, when only one $ML^{3-y\,(out)}$ complex is formed, $I_1^{\circ(out)} \approx I_0^\circ$, the specific intensity for the free M^{3+}; then $I_{mes} \approx I_0^\circ [M]_T$, so that spectrophotometry is not sensitive to complexation at all. However, when $ML^{3-y\,(in)}$ is formed exclusively or in addition to $ML^{3-y\,(out)}$, spectrophotometry is relevant for measuring either $\beta_1^{(tot)} = \beta_1^{(in)}$ or $\beta_1^{(tot)} = \beta_1^{(in)} + \beta_1^{(out)}$, respectively.

Supporting Information Available: MS/MS data and assignments, MS data and assignments in the negative ion mode. This material is available free of charge via the Internet at http://pubs.acs.org.

Footnotes

$ PhD grant from ANDRA.

(1) Bruno, J. Trace Element Modelling. In *Modelling in Aquatic Chemistry*; Grenthe, I.; Puigdomenech, I. Eds; Elsevier Science BV: Amsterdam, 1997.

(2) Clark, D.L.; Hobart, D.E.; Neu, M.P. *Chem. Rev*. **1995**, *95*, 25-48.

(3) Hadermann, J. The pillars of Safety. In *Modelling in Aquatic Chemistry;* Grenthe, I.; Puigdomenech, I. Eds; Elsevier Science BV: Amsterdam, 1997.

(4) Wanner, H. The NEA Thermochemical Data Base project, Report TDB-0.2, OECD Nuclear Energy Agency, Data Bank, France, 1991.

(5) Johnson, L.H.; Shoesmith, D.W. Spent Fuel. In *Radioactive waste forms for the future*; Lutze, W.; Ewing, R.C. Eds.; Elsevier Science Publishers B.V., 1988; Ch. 11, pp.635-698.

(6) (a) Choppin, G.R. *J. Less-Common Metals* **1983**, *93*, 232-330; (b) Krauskopf, K.B. *Chem. Geol*. **1986**, *55*, 323-335.

(7) Robouch, P. Contribution à la prévision du comportement de l'américium, du plutonium et du neptunium dans la géosphère ; données géochimiques. Thesis, Université Louis Pasteur, Strasbourg, France, 1987.

(8) Giffaut, E. Influence des ions chlorure sur la chimie des actinides. Effets de la radiolyse et de la température. Thesis, Université Paris-sud, Orsay, France, 1994.

(9) Silva, R.J.; Bidoglio G.; Rand, M.H.; Robouch, P.B.; Wanner, H.; Puigdomenech, I. *Chemical Thermodynamics of Americium*, Elsevier BV: Amsterdam, 1995.

(10) Guillaumont, R.; Fanghänel, T.; Fuger, J.; Grenthe, I.; Neck, V.; Palmer, D.A.; Rand, M.H. *Update on the Chemical Thermodynamics of Uranium, Neptunium, Plutonium, Americium and Technetium*, Elsevier BV: Amsterdam, 2003.

(11) (a) Wood, S.A. *Chem. Geol*. **1990**, *82*, 159-186; (b) Hendry, M.J.; Wassenaar, L.I. *Water Resour. Res*. **2000**, *36*, 503-513.

(12) Gaucher, E.; Robelin, C.; Matray, J.M.; Négrel, G.; Gros, Y.; Heitz, J.F.; Vinsot, A.; Rebours, H.; Cassagnabère, A.; Bouchet A. *Water Geochemistry and Hydrogeology* **2004**, *29(1)*, 55-77.

(13) Izatt, R.M.; Eatough, D.; Christensen, J.J.; Bartholomew, C.H. *J. Chem. Soc. A* **1969**, 45-47.

(14) Jenkins, I.L.; Monk, C.B. *J. Am. Chem. Soc.* **1950**, *72*, 2695-2698.

(15) Spedding, F.H.; Jaffe, S. *J. Am. Chem. Soc.* **1954**, *76*, 882-884.

(16) Fisher, F.H.; Davis, D.F. *J. Phys. Chem.* **1967**, *71(4)*, 819-822.

(17) Farrow, M.M.; Purdie, N. *J. Solution Chem.* **1973**, *2(6)*, 503-511.

(18) Reidler, J.; Silber, H.B. *J. Phys. Chem.* **1973**, *77(10)*, 1275-1280.

(19) Jones, H.W.; Monk, C.B. *Trans. Faraday Soc.* **1952**, *48*, 929-933.

(20) Aziz, A.; Lyle, S.J. *J. Inorg. Nucl. Chem.* **1970**, *32*, 1925-1932.

(21) Simpson, C.; Matijevic, E. *J. Solution Chem.* **1987**, *16(5)*, 411-417.

(22) Sekine, T. *Acta Chem. Scand.* **1965**, *19*, 1469-1475.

(23) DeCarvalho, R.G.; Choppin, G.G. *J. Inorg. Nucl. Chem.* **1967**, *29*,725-735.

(24) Laurie, S.H.; Monk, B. *J. Chem. Soc.* **1963**, 3343-3347.

(25) Farrow, M.M.; Purdie, N. *J. Solution Chem.* **1973**, *2(6)*, 513-523.

(26) Barnes, J.C. *J. Chem. Soc.* **1964**, 3880-3885.

(27) Hale, C.F.; Spedding, F.H. *J. Phys. Chem.* **1972**, *76(20)*, 2925-2929.

(28) Manning, P.G.; Monk, C.B. *Trans. Faraday Soc.* **1962**, *58*, 938-941.

(29) Aziz, A.; Lyle, S.J.; Naqvi, S.J. *J. Inorg. Nucl. Chem.* **1968**, *30*, 1013-1018.

(30) Bilal, B.A.; Koss, V. *J. Inorg. Nucl. Chem.* **1980**, *42*, 1064-1065.

(31) Bansal, B.M.L.; Patil, S.K., Sharma, H.D. *J. Inorg. Nucl. Chem.* **1964**, *26*, 993-1000.

(32) (a) Bünzli, J.C.G. Luminescent probes. In *Lanthanides Probes in life, Chemical and Earth Science – Theory and Practice*, Bünzli, J.C.G., Choppin, G.R., Eds; Elsevier: Amsterdam, 1989; (b) Moulin, C.; Decambox, P.; Moulin, V.; Decaillon, J.C. *Anal. Chem.* **1995**, *67*, 348-353; (c) Colette, S.; Amekraz, B.; Madic, C.; Berthon, L.; Cote, G.; Moulin, C. *Inorg. Chem.* **2004**, *43*, 6745-6751.

(33) Paviet, P.; Fanghänel, T.; Klenze, R.; Kim, J. I. *Radiochim. Acta.* **1996**, *74*, 99-103.

(34) Neck, V.; Fanghänel, T.; Kim, J. I. *Aquatic Chemistry and thermodynamic modeling of trivalent actinides*, *Wiss. Ber. – Forschungszent. Karlsruhe*, 1-108, 1998.

(35) Grenthe, I.; Fuger, J.; Konings, R.J.M.; Lemire, R.; Muller, A.B.; Nguyen-Trong, C.; Wanner, H. *Chemical Thermodynamics of Uranium*, Elsevier BV: Amsterdam, 1992.

(36) (a) Colette, S.; Amekraz, B.; Madic, C.; Berthon, L.; Cote, G.; Moulin, C. *Inorg. Chem.* **2002**, 41, 7031-7041; (b) Colette, S.; Amekraz, B.; Madic, C.; Berthon, L.; Cote, G.; Moulin, C. *Inorg. Chem.* **2003**, *42*, 2215-2226.

(37) Moulin, C.; Amekraz, B.; Hubert, S.; Moulin, V. *Anal. Chim. Acta* **2001**, *441*, 269-279.

(38) Kebarle, P. *J. Mass Spectrom.* **2000**, *35*, 804-817.

(39) (a) Renaud, F.; Piguet, C.; Bernardinelli, G.; Hopfgartner, G.; Bünzli, J.-C. G. *Chem. Commun.* **1999**, 457-458; (b) Ross, A.R.S.; Ikonomou, M.G.; Orians, K.J. *Anal. Chim. Acta* **2000**, *411*, 91-102; (c) Delangle, P.; Husson, C.; Lebrun, C.; Pécaut, J.; Vottéro P.J.A. *Inorg. Chem.* **2001**, *40*, 2953-2962; (d) Muller, G.; Bünzli, J.-C. G.; Schenk, K. J.; Piguet, C.; Hopfgartner, G. *Inorg. Chem.* **2001**, *40*, 2642-2651.

(40) (a) Blades, A.T.; Jayaweera, P.; Ikonomou, M.G.; Kebarle, P. *Int. J. Mass Spectrom. Ion Processes* **1990**, *101*, 325-336; (b) Stewart, I.I.; Horlick, G. *Anal. Chem.* **1994**, *66*, 3983-3993.

(41) (a) Wilm, M.S.; Mann, M. *Int. J. Mass Spectrom. Ion Processes* **1994**, *136*, 167-180; (b) Wilm, M.S.; Mann, M. *Anal. Chem.* **1996**, *68*, 1-8; (c) Wood, T.D.; Moy, M.A.; Dolan, A.R.; Bigwarfe, P.M.; White, T.P.; Smith, D.R.; Higbee, D.J. *Appl. Spectrosc. Rev.* **2003**, *38*, 187-244.

(42) Lemire, R.; Fuger, J.; Nitsche, H.; Potter, P.; Rand, M.; Rydberg, J.; Spahiu, K.; Sullivan, J.; Ullman, W.; Vitorge, P.; Wanner, H. *Chemical Thermodynamics of Neptunium and Plutonium*, Elsevier BV: Amsterdam, 2001.

(43) Plancque, G.; Moulin, V.; Toulhoat, P.; Moulin, C. *Anal. Chim. Acta*, **2003**, *478*, 11-22.

(44) Grenthe, I.; Plyasunov, A. V.; Spahiu, K. Estimations of Medium Effects on Thermodynamic Data. In *Modelling in Aquatic Chemistry*; Grenthe, I.; Puigdomenech, I. Eds; Elsevier Science BV: Amsterdam, 1997.

(45) Pitzer, K.S. *Activity coefficients in electrolyte solutions*, Pitzer, K.S., Ed.; 2nd edn., CRC Press, 1991.

(46) Wang, H.; Agnes, G.R. *Anal. Chem.* **1999**, *71*, 4166-4172.

(47) Sadowski, P.; Majdan, M. *Monatsh. Chem.* **1995**, *126*, 863-870.

(48) Carnall, W.T. The absorption and fluorescence spectra of rare earth ions in solution. In *Handbook on the Physics and Chemistry of Rare Earth*, North Holland Publishing: Amsterdam, 1976.

(49) $\Delta_1(\varepsilon m) = (\varepsilon_{EuSO_4^+,ClO_4^-} - \varepsilon_{Eu^{3+},ClO_4^-})m_{ClO_4^-} + (\varepsilon_{EuSO_4^+,HSO_4^-} - \varepsilon_{Eu^{3+},HSO_4^-})m_{HSO_4^-} + (\varepsilon_{EuSO_4^+,SO_4^{2-}} - \varepsilon_{Eu^{3+},SO_4^{2-}})m_{SO_4^{2-}} - \varepsilon_{Na^+,SO_4^{2-}} m_{Na^+} - \varepsilon_{H^+,SO_4^{2-}} m_{H^+}$

$\Delta_2(\varepsilon m) = (\varepsilon_{Na^+,Eu(SO_4)_2^-} - \varepsilon_{Na^+,SO_4^{2-}})m_{Na^+} + (\varepsilon_{H^+,Eu(SO_4)_2^-} - \varepsilon_{H^+,SO_4^{2-}})m_{H^+} - \varepsilon_{EuSO_4^+,ClO_4^-} m_{ClO_4^-} - \varepsilon_{EuSO_4^+,HSO_4^-} m_{HSO_4^-} - \varepsilon_{EuSO_4^+,SO_4^{2-}} m_{SO_4^{2-}}$

(50) Offerlé, S.; Capdevila, H.; Vitorge, P. Report CEA-N-2785, 1995.

(51) Choppin, G.R.; Rizkalla, E.N. Solution chemistry of actinides and lanthanides. In *Handbook on the Physics and Chemistry of Rare Earths. Lanthanides/Actinides: Chemistry,* Gschneidner, K.A. Jr.;

Eyring, L.; Choppin, G.R.; Lander, G.H. Eds.; North-Holland: Amsterdam, 1994; Vol. 18, pp.559-590.

(52) Ciavatta, L. *Ann. Chim. (Rome)* **1990**, *80*, 255-263.

(53) Horrocks, W.DeW.; Sudnick, D.R. *J. Am. Chem. Soc.* **1979**, *101:2*, 334.

(54) Kimura, T.; Choppin, G.R.; Kato, Y.; Yoshida, Z. *Radiochim. Acta* **1996**, *72*, 61.

(55) Rizkalla, E.N.; Choppin, G.R. Lanthanides and actinides hydration and hydrolysis. In *Handbook on the Physics and Chemistry of Rare Earths. Lanthanides/Actinides: Chemistry,* Gschneidner, K.A. Jr.; Eyring, L.; Choppin, G.R.; Lander, G.H. Eds.; North-Holland: Amsterdam, 1994; Vol. 18, pp.529-558.

(56) Margerum, D.W.; Cayley, G.R.; Weatherburn, D.C.; Pagenkopf, G.K. *ACS Monograph* **1978**, *174* (Coord. Chem., v2), 1-220.

(57) Eigen, M.; Tamm, K. *Z. Electrochem.* **1969**, *66*, 93, 107.

Table 1. Stepwise formation constants of $LaSO_4^+$, $La(SO_4)_2^-$, $EuSO_4^+$ and $Eu(SO_4)_2^-$ at 25°C.

Method[a]	Medium	I / M	$\log \beta_1$	$\log K_2$	Ref.
			$La^{3+} + SO_4^{2-} \rightleftharpoons LaSO_4^+$	$LaSO_4^+ + SO_4^{2-} \rightleftharpoons La(SO_4)_2^-$	
cal	$HClO_4/(Me_4N)_2SO_4$	0	3.50±0.04	1.85±0.07	13
con	$La_2(SO_4)_3$	0	3.62		14
con	$La_2(SO_4)_3$	0	3.62		15
con	$La_2(SO_4)_3$	0	3.62		16
con	$La_2(SO_4)_3$	0	3.65±0.02		17
ul abs	H_2SO_4	0	3.62		18
pot		0	3.82±0.04		19
ESI-MS	HNO_3/H_2SO_4	I → 0	3.5±0.3		this work
extr	$NaClO_4$	0.5	1.77±0.02	0.89±0.01	20
cal	$HClO_4/NaClO_4$	1	0.8	0.2	21
extr	$NaClO_4$	1	1.45±0.07	1.01±0.08	22
pot	$NaClO_4$	2	1.29±0.04		23
			$Eu^{3+} + SO_4^{2-} \rightleftharpoons EuSO_4^+$	$EuSO_4^+ + SO_4^{2-} \rightleftharpoons Eu(SO_4)_2^-$	
sol		0	3.72		24
ul abs	$Eu_2(SO_4)_3$	0	3.66		25
cal	$HClO_4/(Me_4N)_2SO_4$	0	3.54±0.03	1.78±0.09	13
sp	$NaClO_4$	0	3.35		26
sp		0	3.67±0.01		27
sp	$NaClO_4$	0.046	2.76±0.01	1.26±0.25	27
extr	$NaClO_4$	0	3.56		28
extr	$NaClO_4$	0.05	2.53		28
extr	$NaClO_4$	0.1	2.23		28
extr	$NaClO_4$	0.5	1.88±0.01	0.91±0.02	29
ix	$NaClO_4$	0.5	1.87±0.01	0.86±0.02	29
extr	$NaClO_4$	1	1.54±0.06	1.15±0.06	22
extr	$NaCl$	1	1.53±0.04[b]		30
ix	$NaClO_4$	1	1.57±0.03	0.83±0.06	31
ix	$HClO_4$	1	1.23±0.03	0.47±0.10	31
pot	$NaClO_4$	2	1.37±0.08	0.59±0.10	23
extr	$NaClO_4$	2	1.38±0.06	0.60±0.12	23
TRLIL		I → 0	3.78±0.06	1.5±0.2	this work
	$H_2SO_4/HClO_4$	0.02-0.04	2.90-3.06	1.21-1.26	this work
	$Na_2SO_4/NaClO_4$	0.50-0.59	1.71-1.76	0.82-0.88	this work
	$Na_2SO_4/NaClO_4$	0.60-0.70	1.67-1.72	0.70-0.82	this work
	$Na_2SO_4/NaClO_4$	0.91	1.62	0.62	this work
	$Na_2SO_4/NaClO_4$	1.91-2.10	1.35-1.37	0.86-0.91	this work
	$Na_2SO_4/NaClO_4$	1.51-1.62	1.41-1.43	0.75-0.78	this work

(a) cal = calorimetry, con = conductimetry, ul abs = ultrasonic absorption, pot = potentiometry, extr = solvent extraction, sol = solubility, sp = spectrophotometry, ix = ion exchange.

(b) As the speciation model accounted for $EuSO_4^+$ and $Eu(SO_4)_3^{3-}$, the $\log \beta_1$ value may be influenced by $\log \beta_3$.

Table 2. SIT coefficients at 25°C.

	Value[a] / kg mol^{-1}	Method	Ref.
$\varepsilon_{H^+,ClO_4^-}$	0.14±0.02		42
ε_{H^+,NO_3^-}	0.07±0.01		42
$\varepsilon_{H^+,HSO_4^-}$	0.10±0.06	$\varepsilon_{Na^+,HSO_4^-} + (0.11\pm0.05)$	this work
$\varepsilon_{H^+,SO_4^{2-}}$	-0.03±0.06	$\approx \varepsilon_{Li^+,SO_4^{2-}}$	42
$\varepsilon_{Na^+,HSO_4^{2-}}$	-0.01±0.02		42
$\varepsilon_{Na^+,SO_4^{2-}}$	-0.12±0.06		42
$\varepsilon_{La^{3+},ClO_4^-}$	0.47±0.03	$0.47 < \varepsilon_{Ln^{3+},ClO_4^-} < 0.52$	42
$\varepsilon_{Eu^{3+},ClO_4^-}$	0.49±0.03		
$\varepsilon_{La^{3+},HSO_4^-}$	0.2$_8$±0.1$_4$	$0.186 \, (z/r_{M^{z+}}) - 0.196$ [b]	this work
$\varepsilon_{Eu^{3+},HSO_4^-}$	0.3$_3$±0.1$_4$		
$\varepsilon_{Eu^{3+},SO_4^{2-}}$	0.8$_6$±0.5	from TRLIL data	this work
$\varepsilon_{MSO_4^+,ClO_4^-}$	0.22±0.09	$\approx \varepsilon_{AmSO_4^+,ClO_4^-}$	42
$\varepsilon_{MSO_4^+,HSO_4^-}$	0.2$_0$±0.1$_0$	$\varepsilon_{AmSO_4^+,ClO_4^-} - (0.02\pm0.02)$	this work
$\varepsilon_{LaSO_4^+,SO_4^{2-}}$	-0.1$_5$±0.2$_3$	$0.205 \, (z/r_{M^{3+}}) - 0.331$	this work
$\varepsilon_{EuSO_4^+,SO_4^{2-}}$	-0.1$_4$±0.2$_5$		
$\varepsilon_{Na^+,M(SO_4)_2^-}$	-0.05±0.07	$\approx \varepsilon_{Na^+,Am(SO_4)_2^-}$	42

(a) Uncertainty depends on the estimation method: For analogy, $(\sigma^2+0.05^2)^{0.5}$ kg mol^{-1} where σ is the original uncertainty; for correlation, it is calculated from the standard error of parameters in the linear regression.

(b) Correlation on the basis of ε values calculated from Pitzer parameters:[45] $\varepsilon_{K^+,HSO_4^-}$ = -0.04±0.04, $\varepsilon_{Mg^{2+},HSO_4^-}$ = 0.33±0.05, $\varepsilon_{Ca^{2+},HSO_4^-}$ = 0.12±0.05, $\varepsilon_{Fe^{2+},HSO_4^-}$ = 0.3$_8$±0.1$_1$.

Table 3. Complexes detected by nanoESI-MS for 10^{-3} M and 5×10^{-4} M La(NO$_3$)$_3$ under pH range 1-2 in HNO$_3$/H$_2$SO$_4$ medium.

La^{3+}		LaSO$_4^+$	
[LaOH(H$_2$O)$_n$]$^{2+}$, n=5-7	m/z 123, 132, 141	[La(SO$_4$)(H$_2$O)$_n$]$^+$, n=1-4	m/z 253, 271, 289, 307
[LaO(H$_2$O)$_n$]$^+$, n=0-2	m/z 155, 173, 191	[La(SO$_4$)(H$_2$O)$_n$(HNO$_3$)]$^+$, n=0-3	m/z 298, 316, 334, 352
[LaO(H$_2$O)$_n$(HNO$_3$)]$^+$, n=0-1	m/z 218, 236	[La(SO$_4$)(H$_2$O)$_n$(H$_2$SO$_4$)]$^+$, n=0-4	m/z 333, 351, 369, 387, 405
[La(NO$_3$)$_2$(H$_2$O)$_n$]$^+$, n=0-2	m/z 263, 281, 299	[La(SO$_4$)(H$_2$O)$_n$(H$_2$SO$_4$)$_2$]$^+$, n=1-3	m/z 449, 467, 485

Table 4. Speciation results and measured fluorescence lifetimes of Eu(III) aqueous solutions at 25°C.

[Na$^+$] / M	log K_b	-log[H$^+$]	log[SO$_4^{2-}$]	% of species			τ / µs	N_{H_2O}
				Eu^{3+}	EuSO$_4^+$	Eu(SO$_4$)$_2^-$		
0.00	-	2.00	-	100.0	0.0	0.0	110	9.0
0.50	1.30	3.07	-6.71	100.0	0.0	0.0	113	8.8
1.94	1.15	3.07	-1.98	79.0	19.0	2.0	112	8.9
0.50	1.30	3.09	-2.12	67.4	30.5	2.1	117	8.5
1.89	1.14	3.10	-1.68	63.9	30.0	6.2	113	8.8
0.50	1.29	3.10	-1.94	58.0	38.1	3.9	118	8.4
1.84	1.14	3.13	-1.49	52.1	36.6	11.2	119	8.4
0.50	1.29	3.12	-1.73	45.5	46.8	7.6	120	8.3
0.51	1.29	3.13	-1.66	41.2	49.3	9.5	121	8.2
0.51	1.28	3.17	-1.46	30.3	53.8	15.9	123	8.1
0.52	1.26	3.24	-1.20	19.4	53.7	26.8	126	7.9
0.00	1.65	1.83	-2.22	19.4	74.0	6.6	123	8.1
1.41	1.12	3.40	-0.90	19.3	42.4	38.3	127	7.8
1.30	1.11	3.46	-0.83	16.6	41.5	41.9	129	7.7
0.53	1.23	3.36	-0.98	13.2	49.4	37.4	129	7.7
0.40	1.26	3.35	-1.00	10.9	50.5	38.6	130	7.6
0.55	1.20	3.47	-0.84	10.5	45.4	44.0	132	7.5
0.50	1.18	3.62	-0.70	8.1	41.4	50.4	133	7.4
0.60	1.11	3.89	-0.52	7.9	36.8	55.3	133	7.4

Captions for figures

Figure 1. Dependence of log $K_{b,m}$ with ionic strength, I_m at 25°C. The thin and bold continuous lines represent fits to experimental values (open circles) selected in Refs. 44 and 42, respectively, with a simplified SIT formula for a $NaClO_4$ medium (Eq. 6). Values were also calculated with the SIT formula for each of our solutions accounting for the proportions of ionic constituents (cross and black circles). For comparison, extrapolation of log $K_{b,m}$ to high ionic strengths is shown (dotted line) for a H_2SO_4 medium where HSO_4^- predominates.

Figure 2. NanoESI-MS spectra of 10^{-3} M $La(NO_3)_3$ and a 2-fold molar ratio of SO_4^{2-} at pH 2, HNO_3/H_2SO_4 medium, cone-voltage 30 V.

Figure 3. Interpretation of nanoESI-MS results with the formation of $LaSO_4^+$. Experimental values of log R and log β_1 are represented against log$[SO_4^{2-}]$, calculated using Eqs. 8-9. Thin and bold straight lines result from linear regression analyses of the experimental data for pH 1, $0.10 < I < 0.14$ (■), and pH 2, $0.01 < I < 0.02$ (▲) respectively. Close and open symbols refer to 10^{-3} M and 5×10^{-4} M La(III) solutions, respectively.

Figure 4. TRLIL spectra of Eu(III) with $-4.1 < \log[SO_4^{2-}] < -1.6$, in $Na_2SO_4/NaClO_4$ aqueous solutions with $I = 0.5$ M at $-\log[H^+] > 3$ and 25°C.

Figure 5. TRLIL data analysis at 25°C: (a) normalized relative intensity, I_{norm}^R, at 618 nm against log$[SO_4^{2-}]$, measured for Eu(III) aqueous solutions with different ionic conditions; the theoretical curves are fitted to the data according to three different models (see text): Assuming the formation of $EuSO_4^+$ from Eu^{3+} (model A), and adding $Eu(SO_4)_2^-$ as outer (model B) or outer and inner (model C) complexes; (b) speciation diagrams of Eu(III) for the 3 sets of ionic conditions.

Figure 6. Experimental values of log β_1 against ionic strength, I_m, at 25°C for the formation of $LaSO_4^+$ and $EuSO_4^+$. The data determined in this work (closed symbols) are compared to literature data reported in Table 3 (open symbols). The dependence with I_m is calculated using the simple SIT formula (Eq. 10) and $\varepsilon_{i,j}$ values (Table 2) when $NaClO_4$ (continuous line) or Na_2SO_4 (dotted line) predominates as supporting electrolytes.

Figure 7. TRLIL spectra of Eu^{3+}, $EuSO_4^+$ and $Eu(SO_4)_2^-$ for $\lambda_{excitation} = 395$ nm at 25°C.

Figures

Figure 1.
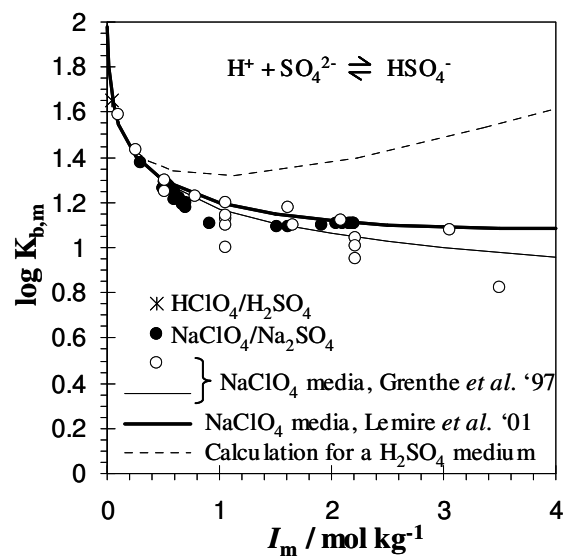
Figure 2.
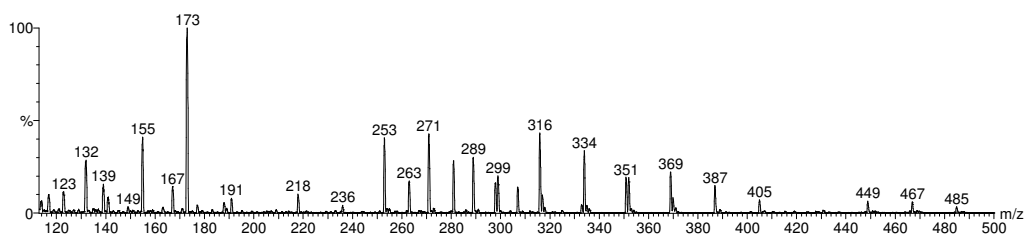
Figure 3.

Figure 4.

Figure 5.

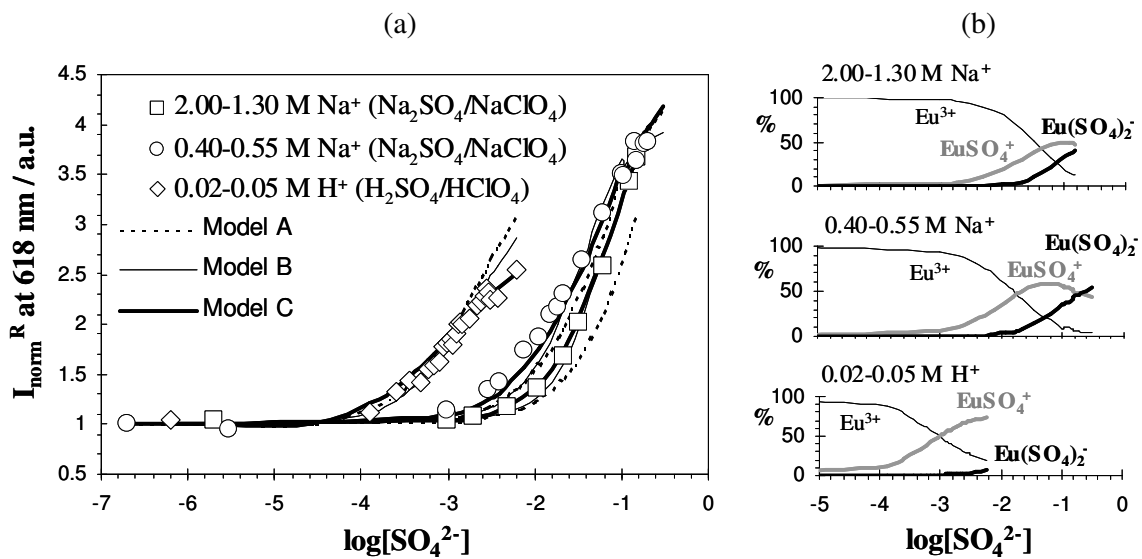(a)   (b)
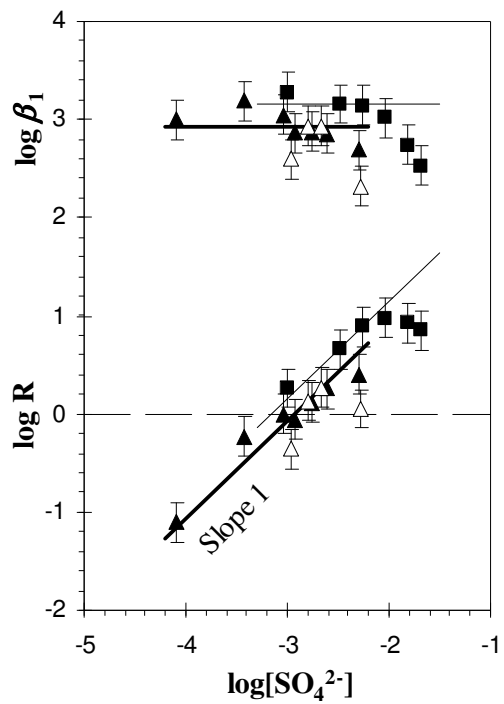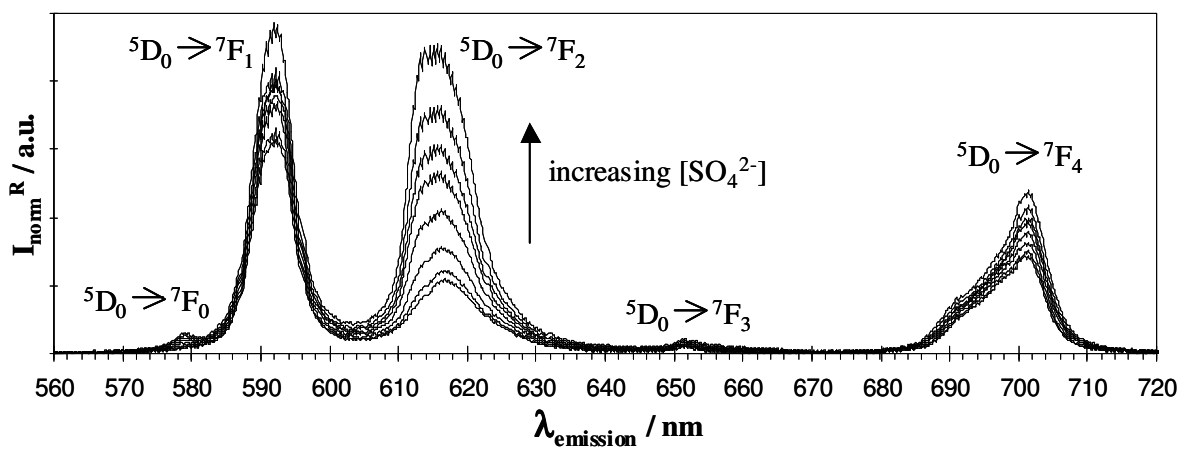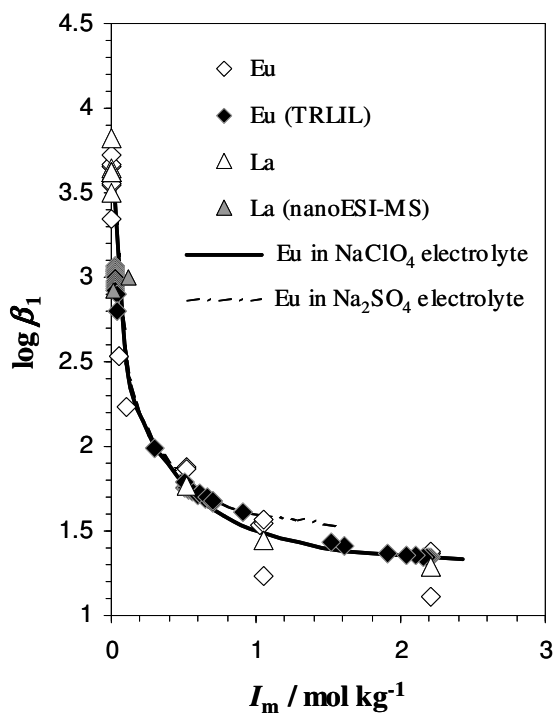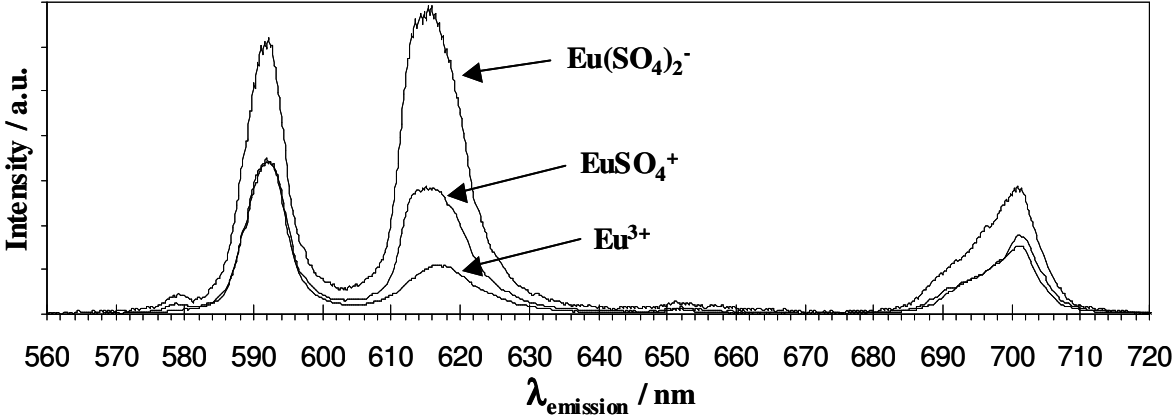

Figure 6.

Figure 7.

Synopsis

Sulphate complexation of lanthanides is of great interest to predict the speciation of radionuclides in natural environments. Thermodynamic constants were measured for the formation of the mono and disulphate complexes of lanthanides(III) by TRLIL for Eu(III) and by nanoESI-MS for La(III). The luminescence analysis of Eu(III) solutions suggested the formation of inner sphere complexes of Ln(III) with monodentate SO_4^{2-}.